Controllable branching of optical beams by quasi-two-dimensional dark spatial solitons

D. Neshev,* A. Dreischuh,* S. Dinev,* and L. Windholz

Technical University Graz, Institute of Experimental Physics, Petersgasse 16, A-8010 Graz, Austria

Received October 23, 1996; revised manuscript received July 2, 1997

A variable number of quasi-two-dimensional dark spatial solitons of adjustable transverse velocities could be generated by a proper choice of the initial phase profile (odd or even) and the width of the crossed dark stripes and the background-beam intensity. The possibility of branching a single input probe beam into ordered structures of subbeams is demonstrated numerically in a bulk self-induced-defocusing Kerr nonlinear media. The energy-density branching efficiency for each subbeam is evaluated and discussed. © 1997 Optical Society of America [S0740-3224(97)04510-4]

1. INTRODUCTION

Dark spatial optical solitons form a specific class of self-supported beams for which the diffraction is compensated by the beam's self-action in media of negative nonlinearities.[1,2] Because of the negative nonlinear refractive-index correction, the refractive index itself appears lower in the dark spatial soliton (DSS) wings compared with its value in the vicinity of the intensity dip. As a consequence, the DSS's should obey guiding properties. The last is confirmed both theoretically and experimentally for one-dimensional (1D) and two-dimensional (2D) DSS's.[3,4] The same should hold also for a quasi-2D DSS formed by two crossed fundamental 1D odd dark spatial solitons (ODSS's).[5] Since the transverse refractive-index distribution is not axially symmetrical in this case, the guiding quality should be analyzed in detail, as it is done in Section 3 of this paper.

Characteristic for the 1D black ODSS is the abrupt π-phase shift at the zero-intensity position.[2,6] The product $I_o a^2$ is found to be a constant for the ODSS's, where I_0 is the background-beam intensity and a is the dark beam width. If the phase jump is absent in the initial phase portrait of the dark formation (i.e., even dark beam), the latter splits thresholdless into complementary pairs of diverging gray 1D ODSS's.[6] An increase in the background-beam intensity also causes splitting of the 1D ODSS, leading to the formation of an on-axis fundamental 1D ODSS and a diverging pair of gray ODSS's.[6]

The splitting of crossed dark formations can be controlled by (i) switching between odd and even dark formations at the entrance face of the nonlinear medium (NLM), for example, by means of programmable writing of synthesized holograms in liquid-crystal spatial light modulators[7]; (ii) by varying the background-beam intensity and/or the initial widths of the odd or even dark formations.

Planar Y junctions are already realized in Kerr[8] and photorefractive[9] nonlinear media. The photovoltaic photorefractive media do not require external electrical fields, and typically, have long lifetimes of the charge-induced refractive-index perturbations.[10] Steering of dark solitons is realized by the adjustment of the difference in the phase between the waves supporting them in both Kerr[11] and saturable nonlinear media.[12] It was recently predicted[13] and confirmed experimentally[14] that the spatial position of an optical vortex soliton with respect to the host background beam could be controlled by a superposition of a second weak coherent background radiation with no azimuthal phase variations.

In this study, we present results supporting the idea that a variable number of quasi-2D ODSS's formed by crossed dark stripes at the entrance of the NLM could cause branching of a single input probe beam into a discrete selectable number of channels (subbeams) and, eventually, with controllable intensity-branching ratios. These problems are discussed in Sections 4 and 5 of this paper.

2. NUMERICAL PROCEDURE AND INITIAL CONDITIONS

Under the slowly varying envelope approximation, the longitudinal evolution of the dark formations in self-defocusing nonlinear media is described by the $(2+1)D$ nonlinear Schrödinger equation (Ref. 15):

$$i\frac{\partial E_D}{\partial z} + \frac{1}{2L_{\mathrm{Diff}}{}^D}\left(\frac{\partial^2}{\partial x^2} + \frac{\partial^2}{\partial y^2}\right)E_D + \frac{1}{L_{\mathrm{NL}}{}^D}|E_D|^2 E_D = 0, \tag{1}$$

where $L_{\mathrm{Diff}} = L_{\mathrm{Diff}}{}^D = k_D a_D{}^2$ and $L_{\mathrm{NL}}{}^D = 1/(k_D n_2{}^{\mathrm{SPM}}|E_D|^2)$ are the Rayleigh diffraction and the nonlinear lengths, respectively, k_D is the wave number for the dark wave, $n_2{}^{\mathrm{SPM}} < 0$ is the nonlinear refractive-index coefficient for self-phase modulation (SPM), and E_D is the normalized background-beam electric-field amplitude. Since either negligible or moderate probe-beam self-action is considered to accompany the induced-phase modulation (IPM) originating from the dark beam, the probe-wave evolution is studied by one's solving the generalized nonlinear Schrödinger equation

0740-3224/97/112869-08$10.00

$$i\frac{\partial E_s}{\partial z} + \frac{1}{2L_{\mathrm{Diff}}{}^{S}}\left(\frac{\partial^2}{\partial x^2} + \frac{\partial^2}{\partial y^2}\right)E_S + \left(\frac{|E_S|^2}{L_{\mathrm{NL}}{}^{S}} + \frac{\alpha|E_D|^2}{L_{\mathrm{NL}}{}^{D}}\right)E_S = 0. \quad (2)$$

In Eq. (2) $L_{\mathrm{Diff}}{}^{S}$ and $L_{\mathrm{NL}}{}^{S}$ are the signal diffraction and the nonlinear lengths, and α accounts for the relative strength of the IPM. Furthermore, in the above notations the transverse spatial coordinates x and y are normalized to the initial transverse extent of the crossed dark formations, i.e., to min $[a_{D_x}(z=0),\ a_{D_y}(z=0)]$. For simplicity $|k_D - k_S| \ll k_{D,S}$ is assumed in this analysis. The four-wave mixing effects occurring in materials possessing fast nonlinearities are not accounted for in model equations (1) and (2). One argument for this is the reduced overlapping between the high-intensity wings of the bright and the dark waves considered. At dark and bright beams at different wavelengths, this simplification holds also for NLM much longer than the coherence length. In media with photorefractive nonlinearities (Section 6), the nonlinear response is too slow to follow the beating between the components of different wavelengths. Additionally, the writing of the quasi-2D DSS structure can precede the branching of the bright wave (i.e., temporal overlapping is absent).

The numerical procedure used for solving Eqs. (1) and (2) is a 2D generalization of the beam-propagation method at $\alpha = 2$. Discretization over 1024×1024 grid points is used for both dark and bright formations analysis. A finite-extent background beam of a super-Gaussian form factor

$$B(r) = \exp[-(r/40)^{12}], \qquad r = (x^2 + y^2)^{1/2} \quad (3)$$

and radius, 40 times larger than the highest width of the 1D dark formations nested in is used. The odd dark stripe at the entrance face of the NLM was described by

$$E_D{}^{O}(x, y, z=0) = E_0 B(r)|\tanh(x)|\exp(i\Phi) \quad (4a)$$

with

$$\Phi(y, z=0) = 0, \qquad x \leqslant 0,$$
$$\Phi(y, z=0) = \pi, \qquad x > 0, \quad (4b)$$

whereas for the even stripe, the description

$$E_D{}^{E}(x, y, z=0) = E_0 B(r)[1 - \mathrm{sech}(x)] \quad (5)$$

is used. The probe beams were assumed to be initially of sech shapes and widths equal to these of the 1D odd dark formations.

Figure 1a is intended to provide an idea of the spatial refractive-index distribution $n = n_0 + n_2{}^{\mathrm{SPM}}|E_D{}^0|^2$ in the vicinity of a quasi-2D odd dark formation imposed on a sufficiently broader background beam. The negative nonlinear refractive-index correction $n_2{}^{\mathrm{SPM}}|E_D{}^0|^2$ causes the well-pronounced decrease of the refractive index in the wings of the crossed dark stripes, thus indicating guiding properties. To evaluate the guiding quality after the branching process is completed, we assumed that an imaginary array of 3×3 information channels (waveguides of rectangular cross sections and typical dimension x_0, four times the diameter of the bright beam at

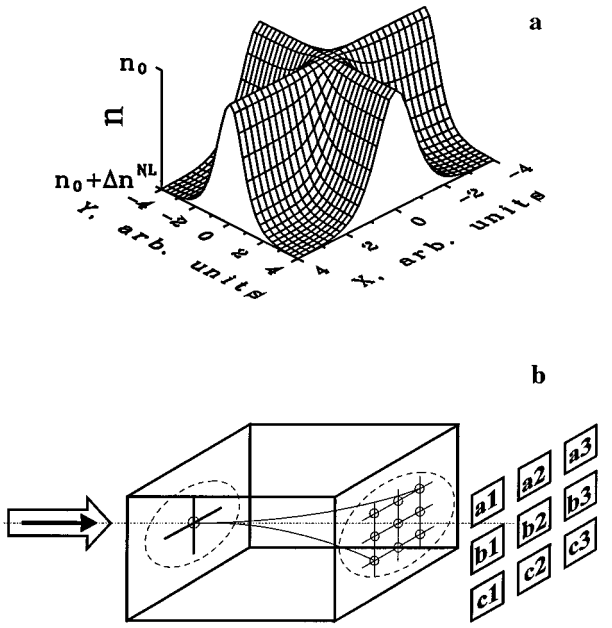

Fig. 1. a, Qualitative spatial refractive-index variation in the vicinity of a quasi-2D odd dark formation at $n_2{}^{\mathrm{SPM}} < 0$. b, Disposition scheme and notation of the imaginary information channels coupled to the exit face of the NLM.

$z = 0$) are coupled to the exit face of the NLM. These channels are spaced at $x_0/2$ and the incoming probe beam is assumed to be aligned on axis with channel b2 (Fig. 1b). Since the $(3+1)D$ spatiotemporal evolution of the probe beam or pulse during the guiding and/or branching does require further extended analysis with respect to the pulse walk-off and the temporal broadening owing to the group-velocity dispersion, this study is far from addressing the particular technical problems of an eventual application, and we mainly emphasize the stationary physical picture of the processes.

3. GUIDING OF SIGNAL BEAMS BY QUASI-TWO-DIMENSIONAL ODD DARK SPATIAL SOLITONS

First, the quasi-2D ODSS is modeled as generated initially by two crossed odd dark stripes, i.e.,

$$E_D(x, y, z=0) = E_D{}^0(x, z=0)E_D{}^0(y, z=0). \quad (6)$$

Since each dark stripe is assumed to satisfy exactly the initial conditions required for the formation of a 1D ODSS (phase discontinuity at the irradiance minimum, zero transverse velocity, and conservation of both the soliton constant and of the total number of the dark structures[2]), no excess of energy (negative) is shaded. Therefore an initiation of a modulational instability is unlikely. Stable propagation of the quasi-2D ODSS's was observed up to $z = 20L_{\mathrm{Diff}}$ (Fig. 2a). Only the wings of the 1D ODSS's were influenced by the finite background-beam spreading.[15] The initially hyperbolic-secant-shaped probe beam was found to be guided successfully by the quasi-2D ODSS (Fig. 2b). The lack of an axial symmetry in the refractive-index variations induced at negligible probe-wave self-action (Fig. 1a) results in an incomplete

guiding of the bright beam along the odd dark stripes and in the formation of a starlike transverse energy-density distribution. A cross section of the probe beam along the odd dark solitons is presented in Fig. 3 (solid curve). For comparison, the dashed curve presents the probe-beam

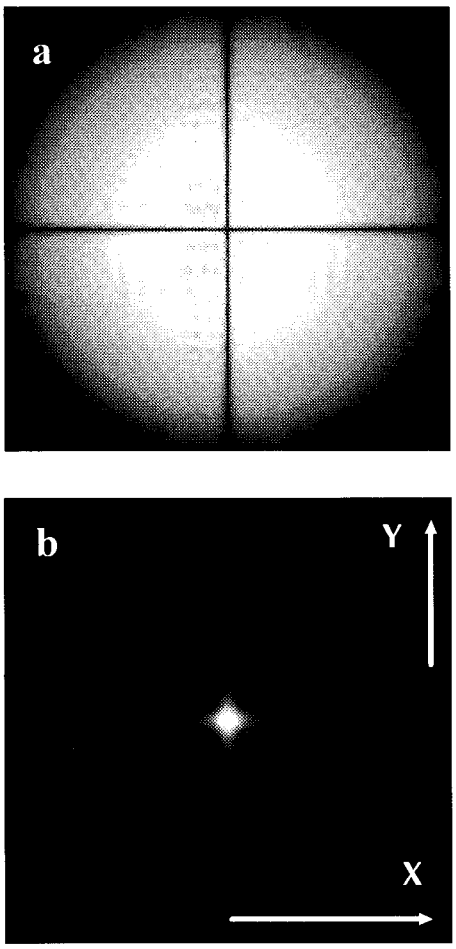

Fig. 2. a, Gray-scale image of the finite-background super-Gaussian beam with the quasi-2D ODSS's nested in after a propagation path length of $z = 20L_{\mathrm{Diff}}$; b, The same for the guided probe wave (twice magnified).

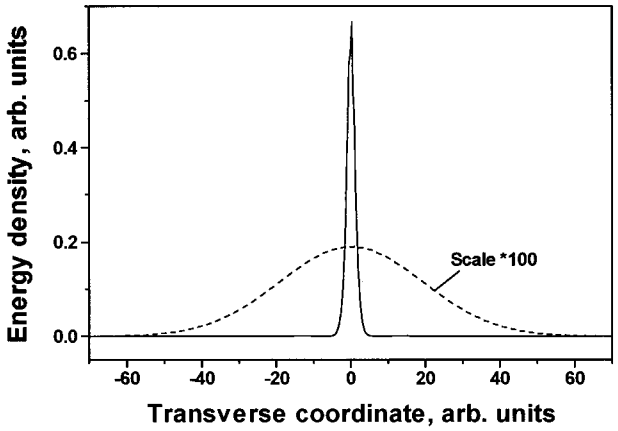

Fig. 3. Cross section of the probe wave from Fig. 2b along the 1D ODSS stripe (solid curve) and the respective energy-density distribution in a linear mode of propagation (dashed curve, scaling factor of 100).

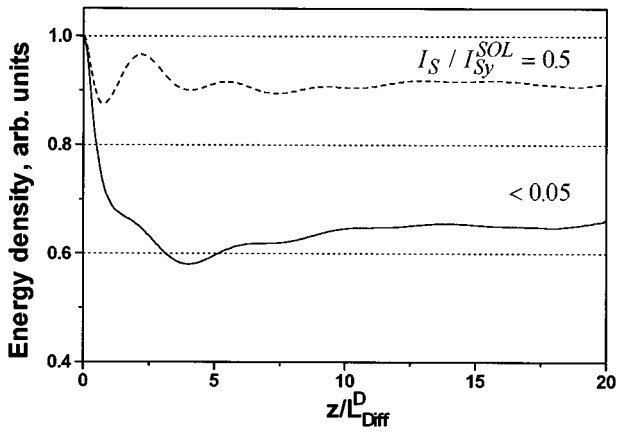

Fig. 4. Evolution of the probe-beam peak energy density along the nonlinear propagation path at negligible (solid curve) and moderate (dashed curve) probe-beam self-action.

profile in the absence of an IPM from the quasi-2D dark formation (i.e., probe-beam evolution influenced by the 2D diffraction only). The estimation has shown that only 2.5% of the energy transmitted to channel b2 [integrated over the channel aperture (Fig. 1b)] becomes redistributed at a negligible cross talk to channels a1, a3, c1, and c3, and with a cross talk of 0.22% to channels a2, c2, b1, and b3 at $z = 20L_{\mathrm{Diff}}$. (This value of the cross-talk signal is of the order of the estimated accuracy during its evaluation). After a relatively rapid decrease in the probe-beam peak intensity up to $z = 1L_{\mathrm{Diff}}$, it tends to stabilize at 64% of its initial value for $z > 8L_{\mathrm{Diff}}$ (Fig. 4, solid curve). If the initial probe-beam intensity is increased to 50% of the intensity required for a 1D bright soliton formation (along the y axis) under probe-beam self-focusing conditions ($I_S = I_{\mathrm{Sy}}^{\mathrm{SOL}}$), the IPM on the dark formation originating from the bright one is found to improve the guiding quality to practically a 100% transmission efficiency to channel b2 [within the estimation accuracy mentioned] (Fig. 1b). The starlike structure in the probe beam appeared weaker when expressed, and the peak intensity was found to asymptotically tend to 91% of its initial value (Fig. 4, dashed curve). Oscillations with a period of $z = 7.5L_{\mathrm{Diff}}$ and up to 40% increase of the probe-wave peak energy density were found when at the entrance of the NLM, the intensity of the bright sech-shaped beam is equal to that required for a 1D bright spatial soliton formation. In the last two cases the quasi-2D odd dark structure appears reshaped because of the IPM from the bright beam; however, no indications for a background modulational instability were found. Note that in the framework of this analysis, the signal-beam guiding by quasi-2D ODSS's is the only regime at which the moderate probe-wave self-action does improve the transmission efficiency of the waveguides induced.

4. SIGNAL-BEAM BRANCHING BY CROSSED ONE-DIMENSIONAL ODD AND EVEN DARK SOLITON STRIPES

The characteristic for this interaction configuration is that the 1D even dark stripe does split (even at low back-

ground intensity) into two diverging gray spatial solitons. The initial condition was set numerically to

$$E_D(x, y, z = 0) = E_D{}^0(x, z = 0)E_D{}^E(y, z = 0), \quad (7)$$

i.e., the two gray ODSSs appear separated in a vertical direction [along the y axis, (Fig. 2a)]. The transverse velocity λ_y of these gray solitons is actually the transverse velocity of the quasi-2D DSS. In the absence of interaction with the background wings, it depends on the initial even dark stripe width as $\lambda_y = \cos(2\lambda_y \gamma a_{Dy})$ with γ depending on the linear and the nonlinear refractive indices and the background wavelength.[1,2] In Fig. 5 we present three slices of the branched probe beam at $z = 20L_{\mathrm{Diff}}$ extracted along the fundamental 1D ODSS. The solid curve corresponds to $a_{D_y}(z = 0) = a_{D_x}(z = 0)$, whereas the dashed and the point-dashed curves correspond to $a_{D_y}(z = 0)/a_{D_x}(z = 0)$ equal to 1.5 and 0.5, respectively. In all the three cases a perfect linearity of the quasi-2D DSS positions versus nonlinear propagation path length was found. At no probe-beam self-action the increase in the quasi-2D DSS transverse velocity results in a decrease in the contrast of the quasi-2D branched and guided bright subbeam with respect to the on-axis 1D guided portion of the probe wave (Fig. 5). The estimated values for the energy guided to the information channels a2 (and c2) exceed 11.5, 6.9, and 1.5 times the energy directed to the b2 channel at $a_{D_y}(z = 0)/a_{D_x}(z = 0) = 1.5$, 1, and 0.5, respectively. The branching process completes at approximately $2.5L_{\mathrm{Diff}}$, and the profiles given in Fig. 5 represent the numerical result at $z = 20L_{\mathrm{Diff}}$. The increase in the intensity of the on-axis peak (Fig. 5, point-dashed curve) should be attributed to the relatively high transverse velocity of the quasi-2D DSSs, resulting in incomplete branching and guiding. These results are indicative that a controllable 1:2 and 1:3 probe-wave branching is feasible by adjusting the width of the incoming 1D even dark stripe only. Particular 1D experimental confirmation of these results can be found in Refs. 8 and 9, where the splitting of 1D even dark formations has led to the formation of a Y-junction splitter. The oscillations on the background beam developed during the formation of the gray odd soliton pair served as perturbations causing modulational instability and leading to the generation of pairs of optical vortex solitons (OVS's) of opposite topological charges.[4] This is clearly seen in Fig. 6 [$z = 20L_{\mathrm{Diff}}$ and $a_{D_y}(z = 0)/a_{D_x}(z = 0) = 0.5$] and was observed in all the three cases discussed above. A detailed investigation of this instability is presented in Ref. 16. Even more dramatic results[17] occur when polarization effects are present. The vortices observed, however, did not remarkably influence the splitting and the guiding of the probe wave in the quasi-2D nonlinear waveguide.

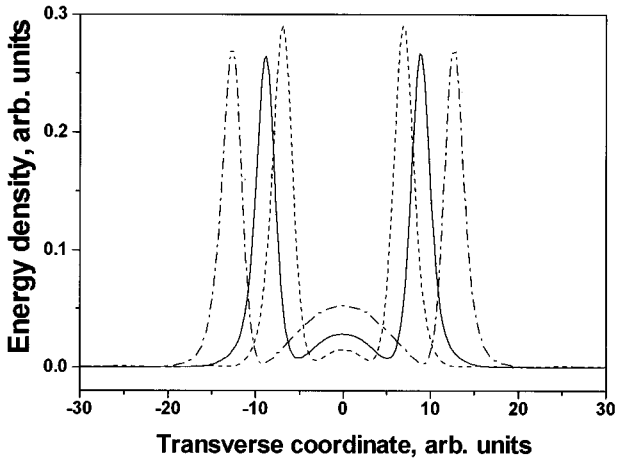

Fig. 5. Cross section of the branched probe beam along the 1D ODSS stripe at $a_{D_y}(z = 0)/a_{D_x}(z = 0) = 0.5$ (point-dashed curve), 1.0 (solid curve), and 1.5 (dashed curve) after nonlinear propagation path length $z = 20L_{\mathrm{Diff}}$.

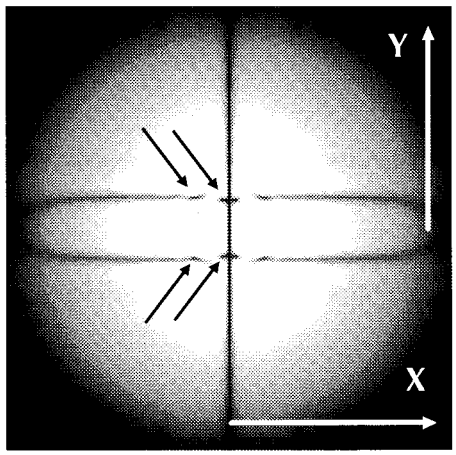

Fig. 6. Gray-scale image of the quasi-2D ODSSs generated from crossed black odd and pair of gray odd DSSs at $a_{D_y}(z = 0)/a_{D_x}(z = 0) = 0.5$. Some of the OVS pairs formed are denoted with arrows.

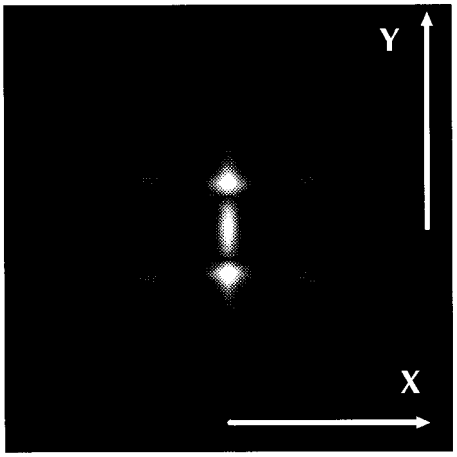

Fig. 7. Branching of a bright probe beam into three subbeams under a nonnegligible self-action. (See the text and Fig. 8 for details.)

In the presence of a moderate probe-wave self-action under self-focusing conditions, the probe-beam branching by crossed 1D even and odd dark stripes is found to be sensitive to the initial even dark stripe width $a_{D_y}(z = 0)$. Let us assume that the probe-beam intensity is high enough to lead to a formation of a 1D bright spatial soliton (in the nonlinear waveguide induced by the 1D ODSS along the y axis), for example, at $a_{S_x}(z = 0)$

$= a_{D_x}(z = 0)$. The increase of the even dark stripe width $a_{D_y}(z = 0)$ by a factor of 1.5 is found to lead to a signal-beam splitting into three channels (Fig. 7) with a side- to central-peak intensity ratio of 1:2 (Fig. 8, dashed curve). By decreasing $a_{D_y}(z = 0)$ three times, one can significantly increase the transverse velocity λ_y of the gray soliton pair (and of the quasi-2D dark formations), thus decreasing the energy coupling efficiency to the side-lying channels a2 and c2 to 0.01 of the respective value for the on-axis channel b2 (Fig. 8, solid curve). In both cases, no substantial energy was coupled to the OVSs generated by the modulational instability of the gray soliton stripes. This way, a controllable branching of a probe beam into 2 and 3 channels with adjustable peak-to-peak intensity ratio seems feasible.

Until now, we assumed that the 1D odd dark formation propagates in the form of a fundamental 1D ODSS. It is known that at increased background intensity, this formation evolves into a fundamental 1D ODSS and a diverging pair of gray ODSS's.[6] Figure 9a shows a simulated gray-scale image in which the vertical odd dark stripe is evolved up to $z = 20L_{\mathrm{Diff}}$ as described. Besides the two quasi-2D ODSS's diverging along the 1D ODSS stripe, four additional quasi-2D dark formations form and diverge radially. In a certain sense their formation could be considered as resulting from collisions of the gray 1D ODSS's without forming bound states.[18] These six quasi-2D waveguides appear able to split the incoming probe beam into six distinct subbeams (Fig. 9b). The estimated energy branching efficiencies are 35% for channels a2 and c2, 3.7% for channels a1, a3, c1, and c3, and 6.6% for the on-axis channel b2. The corresponding energy-density distributions of the branched probe beam along the x and the y axes are presented in Fig. 10 with dashed and solid curves, respectively. In the generation of Figs. 9a, 9b, and 10, the quantity $|E_D{}^0(z = 0)|^2$ was chosen to exceed 1.25 times the value required for the fundamental 1D ODSS formation at $a_{D_x} = 5a_{D_y}$. It was confirmed numerically that the spatial position of the four bright subbeams branched in a diagonal direction could be controlled by varying the background-beam intensity

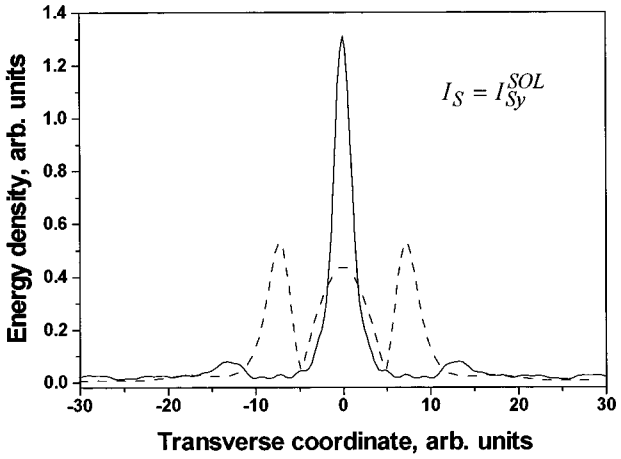

Fig. 8. Branching of the probe wave into three channels with adjustable peak-to-peak energy-density ratio by varying the transverse velocity of the gray solitons at $a_{D_y}(z = 0)/a_{D_x}(z = 0) = 0.5$ (solid curve) and 1.5 (dashed curve).

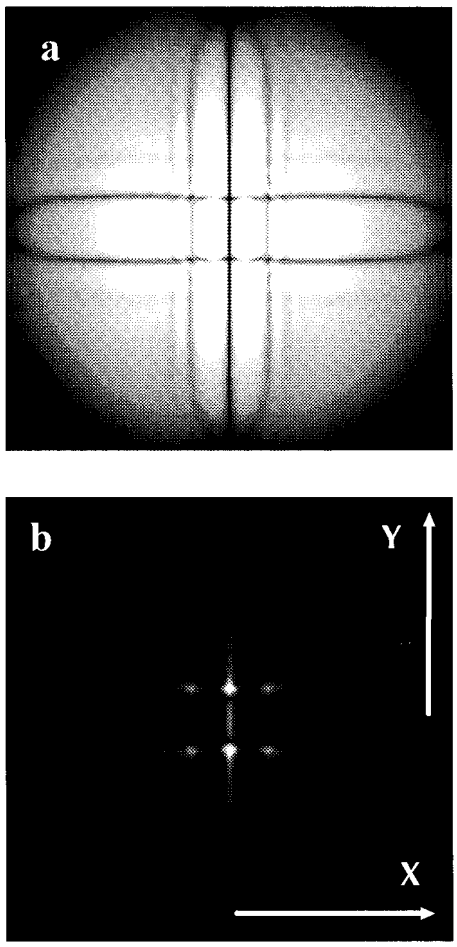

Fig. 9. a, Gray-scale image of a pair of gray ODSSs crossed by a fundamental black ODSS and satellite pair of gray ODSSs ($z = 20L_{\mathrm{Diff}}$, $|E_D{}^0(z = 0)|^2 a_{D_x}{}^2 = 31.25$). b, Probe-beam branching into six subbeams.

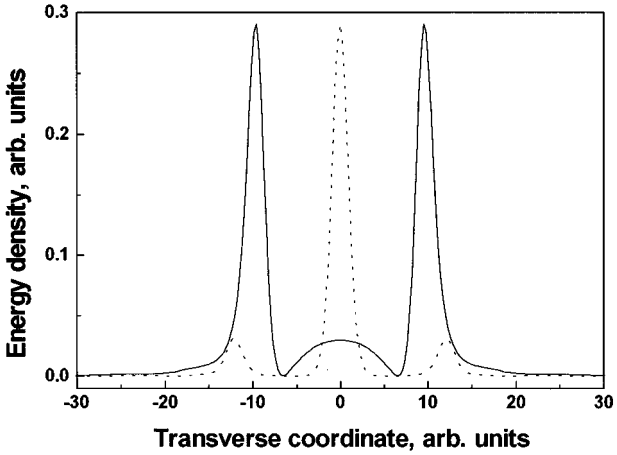

Fig. 10. One-dimensional energy-density probe-field distribution along the x (dashed curve) and y axis (solid curve) extracted from Fig. 9b.

and/or the initial width of the dark stripes. In view of the above, controllable probe-beam branching into six subbeams seems also feasible due to its being insensitive

to the modulational instability that results in the generation of multiple OVS pairs up to the length of propagation $z = 20L_{\mathrm{Diff}}$, which we reached in our simulations.

5. BRANCHING AND GUIDING BY CROSSED ONE-DIMENSIONAL DARK SPATIAL SOLITONS OF THE SAME TYPE

Let us first assume that two crossed even dark stripes enter the NLM and that each of them evolves in a diverging pair of gray 1D ODSS's. This picture does correspond to an initial electric-field amplitude distribution of the type

$$E_D(x, y, z = 0) = E_D{}^E(x, z = 0)E_D{}^E(y, z = 0). \quad (8)$$

Figure 11a presents the probe-wave energy-density distribution at $z = 20L_{\mathrm{Diff}}$ at $a_{D_y}(z = 0) = a_{D_x}(z = 0)$ and $|E_D{}^E(z = 0)|^2\, a_{D_x}{}^2 = 1$. As expected, the four quasi-2D DSS's formed to branch and guide successfully approximately 21.5% of the total probe-beam energy with 13% of the initial probe-wave peak energy density in each channel. One-dimensional cross sections of the branched beam along the gray stripes is shown in Fig. 11b. It was found that a 50% increase in the width of the initial even formations and the associated decrease of their transverse velocity results in a 2.5% enhancement in the energy of each branched subbeam at the expense of more pronounced central and side-wing oscillations. In turn, a 50% decrease of both $a_{D_x}(z = 0)$ and $a_{D_y}(z = 0)$ results in an incomplete branching of the signal, in a reduction of approximately 15% of the subbeam peak energy density, and in each subbeam carrying an estimated 8% of the total incoming probe-wave energy. The eventual probe-wave spatial self-action was found also to influence the process negatively.

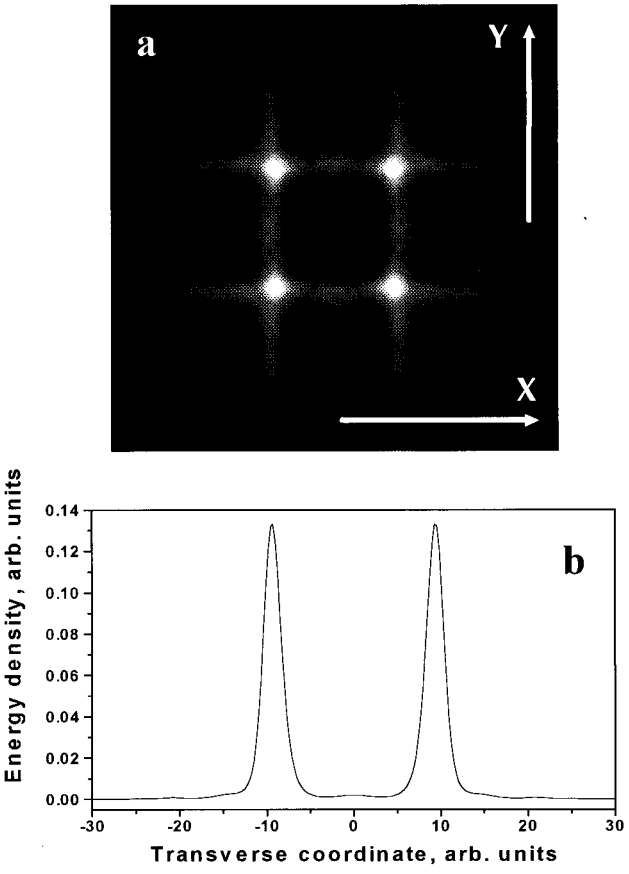

Fig. 11. a, Gray-scale plot and 1D energy-density distribution along the x (y) axis, b, of four subbeams split and guided by pairs of gray ODSS's. (See the text for details.)

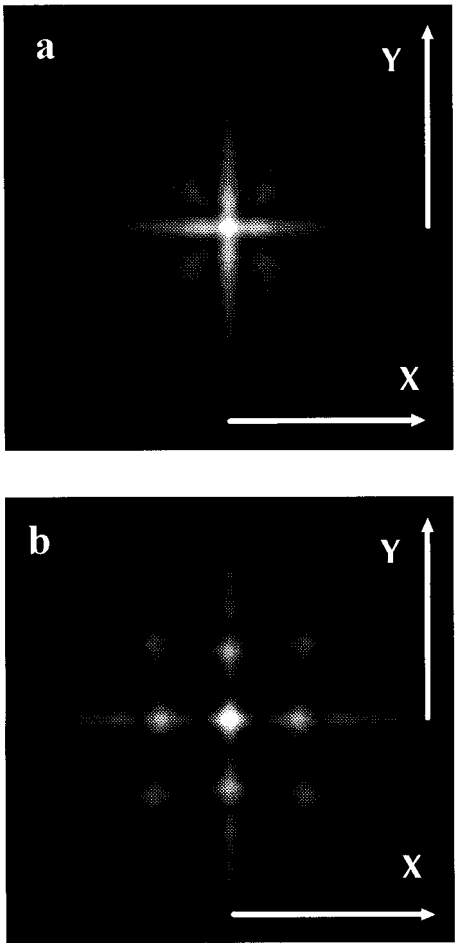

Fig. 12. Gray-scale image of the probe wave branched by crossed higher-order 1D ODSSs (a, $z/L_{\mathrm{Diff}} = 10$; and b, $z/L_{\mathrm{Diff}} = 20$; $|E_D{}^0(z = 0)|^2\, a_{D_x}{}^2 = 31.25$).

The last possibility examined in this work was to use a pair of crossed 1D odd dark stripes nested on a high-intensity background beam. Each of these stripes does evolve into a fundamental 1D ODSS and a diverging pair of gray ones. In the particular case of $|E_D{}^0(z = 0)|^2 = 1.25$ and $a_{D_x}(z = 0) = a_{D_y}(z = 0) = 5$, the narrowing of the incoming dark stripes at the initial stage of the gray soliton pairs formation causes probe-wave splitting and guiding mainly along the fundamental 1D ODSS's (Fig. 12a, $z = 10L_{\mathrm{Diff}}$). Nevertheless, the probe beam seems to branch into nine subbeams at $z = 20L_{\mathrm{Diff}}$ (Fig. 12b). The probe-beam energy redirected to each one of the channels a1, a3, c1, and c3 is approximately 2% of that transmitted to the on-axis channel b2. The same quantity for the channels a2, c2, b1, and b3 was estimated to be 18%. The one-dimensional energy-density distribution along the b1, b2, and b3 channels is plotted in Fig.

13. Besides the outerwing satellites guided by the fundamental 1D ODSS, the branched peaks guided by the quasi-2D ODSS's are of a good contrast.

It was found numerically that the enhancement in $|E_D{}^0(z = 0)|^2$ $a_{D_x}{}^2$ does influence the branching differently, depending on whether the background intensity or the stripe width is increased predominantly. The relative larger increase in $|E_D{}^0(z = 0)|^2$ [up to 2 at $a_{D_{x,y}} = 4$ (Fig. 14a)] causes more pronounced spreading of the background beam and formation of a larger number of OVS pairs. Besides this, the contrast in the branched probe subbeams is better at the expense of a lower-energy efficiency in each channel [especially in channels a1, a3, c1, and c3 (Fig. 14a)] with respect to the case of a predominant enhancement in the initial odd dark stripe width $a_{D_{x,y}}{}^0(z = 0)$ [up to 8 at $|E_D{}^0(z = 0)|^2 = 1$ (Fig. 14b)]. Since the relative energy redirected to channels a2, c2, b1, and b3 is approximately 11% of that directly transmitted to the on-axis channel b2 (Fig. 14a), this situation could be considered as probe-beam branching into five subbeams. Note also that the angular offset between the subbeams is less sensitive to the $a_{D_{x,y}}$ of the odd stripe as compared with the background intensity.

6. CONCLUSION

In view of the results presented, the controllable branching and guiding of probe beams by quasi-2D dark spatial solitons in a discrete, variable number of subbeams appears feasible. The effects discussed are based on Kerr-type solitons. If such quasi-2D dark solitons are written as photorefractive ones, as done in one transverse dimension,[19] the low power needed to do that and their ability to guide powerful beams at nonphotosensitive wavelengths[20] will open the way for constructing practically applicable reconfigurable branchers. The stability of the branching scheme in saturable nonlinear media requires further analyses, since the drift instability can transform each black soliton into a gray soliton and radiation.[21,22] Within the range of the model parameters considered and in a Kerr nonlinear media, the additional OVSs generated did not interact remarkably with the quasi-2D DSS's. It is shown, however, that in a saturable self-defocusing NLM (Kerr-type[23] or photorefractive[24,25]), the snake instability of the dark stripes results in their periodic bending and breaking into sets of vortices. The vortex dynamics in a nonlocal anisotropic NLM is characterized by anisotropy-induced stretching and alignment effects.[26] In view of the different possibilities of the instability dynamics, special attention in the future analyses should be paid to the branching quality of the bright beam. The polarization characteristics of the waves could be expected to also play an important role and to require detailed investigations.

It should appear possible to couple each of the channels (Fig. 1b) to a separate optical fiber of a suitably chosen length. By independently fast modulating the transmission of each channel from 1 to 0 and vice versa and by a subsequent multiplexation of the pulses into a single optical fiber, one can ensure ordering of bright pulses with arbitrary intensities in trains (of binary-coded bits), thus reducing the interaction strength within the consecutive pulses of short durations.[27,28] The realization of this idea requires detailed analysis on the temporal behavior of the

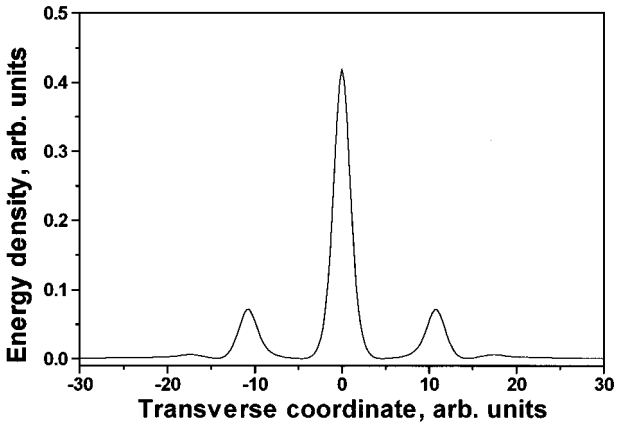

Fig. 13. Probe-wave energy-density distribution along the b1, b2, and b3 (e.g., along the a2, b2, and c2) channel extracted from Fig. 12b.

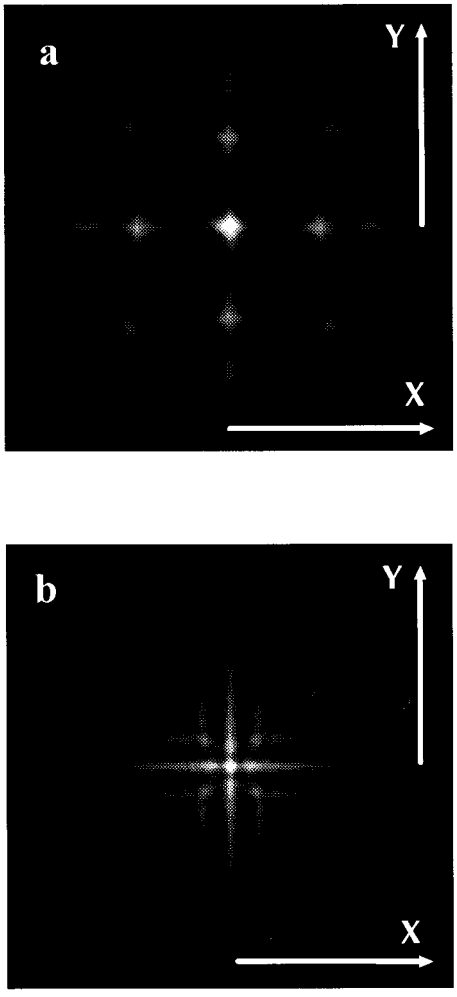

Fig. 14. Same as in Fig. 12, a, at $z/L_{\mathrm{Diff}} = 20$ and $|E_D{}^0(z = 0)|^2 = 2$, $a_{D_x}{}^2 = 4$, $a_{S_{x,y}}{}^2 = 1$; and b, at $E_D{}^0(z = 0)|^2 = 1$, $a_{D_x}{}^2 = 8$, $a_{S_{x,y}}{}^2 = 1$.

probe wave during the branching or guiding process, but it may appear fruitful for maintaining binary-coded information for launching in high bit-rate optical communication systems.

ACKNOWLEDGMENTS

D. Neshev, A. Dreischuh, and S. Dinev are grateful to the Technical University Graz, Institute for Experimental Physics, for the warm hospitality and the exciting scientific atmosphere during their research stays that were supported by the Österreichischer Akademischer Austauschdienst, Austria and by the CEEPUS Network (A-21). A. Dreischuh thanks the Alexander von Humboldt Foundation for the possibility of completing this analysis in the fruitful atmosphere at the Max Planck Institute for Quantum Optics (Garching, Germany). This work was supported by the National Science Foundation, Bulgaria, under contract F-424/1994.

*Permanent address: Sofia University, Department of Quantum Electronics, 5, J. Bourchier Boulevard, BG-1164 Sofia, Bulgaria.

REFERENCES

1. V. Zakharov and A. Shabat, "Interactions between solitons in a stable medium," Zh. Eksp. Teor. Fiz. **64**, 1627 (1973) [Sov. Phys. JETP **37**, 823 (1973)].
2. G. Allan, S. Skiner, D. Andersen, and A. Smirl, "Observation of fundamental dark spatial solitons in semiconductors using picosecond pulses," Opt. Lett. **16**, 156 (1991); D. Andersen, D. Hooton, G. Swartzlander, Jr., and A. Kaplan, "Direct measurements of the transverse velocity of dark spatial solitons," Opt. Lett. **15**, 783 (1990).
3. R. Jin, M. Liang, G. Khitrova, H. Gibbs, and N. Peyghambarian, "Compression of bright optical pulses by dark solitons," Opt. Lett. **18**, 494 (1993); W.-H. Cao and Y.-W. Zhang, "The effect of pulse walkoff on the compression of bright optical pulses by dark solitons," Opt. Commun. **128**, 23 (1996).
4. G. Swartzlander, Jr. and C. Law, "Optical vortex solitons observed in Kerr nonlinear media," Phys. Rev. Lett. **69**, 2503 (1992).
5. G. Swartzlander, Jr., D. Andersen, J. Regan, H. Yin, and A. Kaplan, "Spatial dark soliton stripes and grids in self-defocusing materials," Phys. Rev. Lett. **66**, 1583 (1991).
6. W. Tomlinson, R. Hawkins, A. Weiner, J. Heritage, and R. Thurston, "Dark optical solitons with finite width background pulses," J. Opt. Soc. Am. B **6**, 329 (1989).
7. A. Marrakchi, S. Habiby, and J. Wullert II, "Generation of programmable coherent source arrays using spatial light modulators," Opt. Lett. **16**, 931 (1991).
8. B. Luther-Davies and Y. Xiaoping, "Waveguides and Y-junction formed in bulk media by using dark spatial solitons," Opt. Lett. **17**, 496 (1992).
9. M. Taya, M. Bashow, M. Fejer, M. Segev, and G. Valley, "Y-junctions arising from dark-soliton propagation in photovoltaic media," Opt. Lett. **21**, 943 (1996).
10. M. Taya, M. Bashow, M. Fejer, M. Segev, and G. Valley, "Observation of dark photovoltaic spatial solitons," Phys. Rev. A **52**, 3095 (1995).
11. B. Luther-Davies and X. Yang, "Steerable optical waveguides formed in self-defocusing media by using dark spatial solitons," Opt. Lett. **17**, 1755 (1992).
12. W. Krolikowski, X. Yang, B. Luther-Davies, and J. Breslin, "Dark soliton steering in a saturable nonlinear medium," Opt. Commun. **105**, 219 (1994).
13. J. Christou, V. Tikhonenko, Yu. Kivshar, and B. Luther-Davies, "Vortex soliton motion and steering," Opt. Lett. **21**, 1649 (1996).
14. V. Tikhonenko and N. Akhmediev, "Excitation of vortex solitons in a Gaussian beam configuration," Opt. Commun. **126**, 108 (1996).
15. Yu. Kivshar and X. Yang, "Dark solitons on backgrounds of finite extent," Opt. Commun. **107**, 93 (1994).
16. C. Law and G. Swartzlander, Jr., "Optical vortex solitons and the stability of dark soliton stripes," Opt. Lett. **18**, 586 (1993).
17. C. Law and G. Swartzlander, Jr., "Polarization optical vortex solitons: instabilities and dynamics in nonlinear media," Chaos Solitons Fractals **4**, 1759 (1994).
18. R. Thurston and A. Weiner, "Collisions of dark solitons in optical fibers," J. Opt. Soc. Am. B **8**, 471 (1991).
19. Z. Chen, M. Mitchel, and M. Segev, "Steady-state photorefractive soliton-induced Y-junction waveguides and high-order dark spatial solitons," Opt. Lett. **21**, 716 (1996).
20. M. Morin, G. Duree, G. Salamo, and M. Segev, "Waveguides formed by quasi-steady-state photorefractive spatial solitons," Opt. Lett. **20**, 2066 (1995).
21. Yu. Kivshar and W. Krolikowski, "Instabilities of dark solitons," Opt. Lett. **15**, 1527 (1995).
22. Yu. Kivshar and V. Afanasjew, "Drift instability of dark solitons in saturable media," Opt. Lett. **21**, 1135 (1996).
23. V. Tikhonenko, J. Christou, B. Luther-Davies, and Yu. Kivshar, "Observation of vortex solitons created by the instability of dark soliton stripes," Opt. Lett. **21**, 1129 (1996).
24. A. Mamaev, M. Saffman, D. Z. Anderson, and A. Zozulya, "Propagation of light beams in anisotropic nonlinear media: from symmetry breaking to spatial turbulence," Phys. Rev. A **54**, 870 (1996).
25. A. Mamaev, M. Saffman, and A. Zozulya, "Propagation of dark stripe beams in nonlinear media: snake instability and creation of optical vortices," Phys. Rev. Lett. **76**, 2262 (1996).
26. A. Mamaev, M. Saffman, and A. Zozulya, "Vortex evolution and bound pair formation in anisotropic nonlinear optical media," Phys. Rev. Lett. **77**, 4544 (1996).
27. I. Uzunov, V. Stoev, and T. Tzoleva, "*N*-soliton interaction in trains of unequal soliton pulses in optical fibers," Opt. Lett. **17**, 1417 (1992).
28. A. Berntson, D. Anderson, and M. Lisak, "Analysis of coherent and incoherent interactions of amplitude shifted solitons in optical fibers," Phys. Scr. **52**, 544 (1995).